FMCW Radar-Based Monitoring of Canine Vital Signs Validated Using IMU

天野, 里奈 / Amano, Rina

(出版者 / Publisher)
法政大学大学院情報科学研究科
(雑誌名 / Journal or Publication Title)
法政大学大学院紀要. 情報科学研究科編
(巻 / Volume)
19
(開始ページ / Start Page)
1
(終了ページ / End Page)
9
(発行年 / Year)
2024-03-24
(URL)
https://doi.org/10.15002/00030601

FMCW Radar-Based Monitoring of Canine Vital Signs Validated Using IMU

Rina Amano
Graduate School of Computer and Information Sciences
Hosei University
Tokyo 184-8584, Japan
rina.amano.5p@stu.hosei.ac.jp

***Abstract*—Monitoring the respiratory rate (RR) and heart rate (HR) of canines is of paramount importance for assessing their overall health and well-being. This study introduces a processing pipeline designed to accurately estimate dogs' RR and HR using Frequency-Modulated Continuous Wave (FMCW) radar technology. Unlike previous work, we use a respiration harmonics removal step to enhance the estimated heart rates for dogs. An Inertial Measurement Unit (IMU)-based vital signs monitoring is then validated against reference instruments and used later as ground truth to evaluate the radar-based performance. Extensive experiments were conducted on a diverse set of dog subjects, which included a wide range of breeds, sizes, and ages, thereby ensuring the applicability of the findings across different dog populations. The outcomes of the study achieved an average error of 2.40 bpm for RR and 6.90 bpm for HR from 50cm distance. Furthermore, the research also yielded impressive results at an increased distance of 100 cm, with an average error of 2.58 bpm for RR and 7.70 bpm for HR. These findings underscore the potential of this contactless, radar-based approach to enhance the management of canine health and welfare.**

***Index Terms*—FMCW radar, IMU, vital signs, dog, respiration rate, heart rate, respiration harmonics, healthcare.**

I. Introduction

The rise in dog ownership poses a challenge, as dogs cannot communicate their well-being, making it hard for owners to identify health issues promptly. With a general lack of awareness about vital sign values such as respiration rate and heart rate, as well as baseline health conditions, it's crucial for owners to familiarize themselves with standard health indicators and monitor for deviations. This practice is vital for both owners and veterinarians, offering continuous insights into symptoms and enabling early disease detection.

Apart from invasive techniques like Electrocardiogram (ECG), researchers have explored non-invasive strategies for monitoring vital signs in dogs. Sensors such as inertial measurement units (IMUs) [1]–[3] and radar systems [4], [5] have been used, with IMU sensors providing comfort and ease of use due to their compact size and light weight. Furthermore, radar systems offer more comfort than IMUs, as they remove the necessity for direct contact with the subject dog. Leveraging surface skin vibrations, radar proves effective in extracting information about both respiration and heartbeats.

The challenges encountered when using radar for dogs' vital signs measurement stem from several factors. First, the difficulty in acquiring a reliable standard for vital signs has deterred many studies from effectively evaluating their outcomes against a definitive reference point. Secondly, the challenges associated with experiments involving dogs often lead researchers to resort to anesthesia for controlling dogs' movement, impacting the overall health of the animals. Additionally, the use of small cages to restrict movement, while common, may not accurately reflect real-world scenarios. Moreover, numerous studies have been constrained by a limited number of dog subjects, posing challenges for a comprehensive evaluation since vital sign characteristics vary based on factors such as size, breed, and age. To address these challenges, three research questions are explored. (1) How can a suitable reference be provided to evaluate radar measurement of a dogs' heart rate? (2) What strategies can enhance the accuracy of radar-based heart rate measurements? And, (3) to what range can the proposed solution/method measure heart rate with acceptable accuracy?

To answer these questions, this research proposes a Frequency Modulated Continuous Wave (FMCW) radar-based solution for effectively monitoring the respiratory rate and heart rate of dogs. The approach involves the design of a vital sign monitoring pipeline, leveraging filters for signal extraction and Fast Fourier Transform (FFT) for estimating the rates of vital signs. Unlike previous studies, this research includes a step for removing the impact of respiratory harmonics to improve the performance of heart rate estimation. Subsequently, this method was implemented with IMU to monitor dogs' vital signs, evaluating the outcomes by comparing them to reference devices such as a respiratory belt and ECG. Given that both IMU and radar measure body surface displacement, the same pipeline is applied to estimate respiration and heart rates from radar data. To ensure a thorough evaluation, a series of experiments are conducted involving multiple dogs at varying distances, aiming to validate the effectiveness and reliability of our proposed methodology. To summarize, this research makes the following major contributions:

- Introducing an improved canine vital signs estimation method based on the integration of a breathing harmonics removal stage
- Validating the use of IMU as a reference for assessing radar-based vital signs estimation of canines
- Achieving an average error of 2.40 bpm for RR and

Supervisor: Prof. Jianhua Ma

6.90 bpm for HR from a 50cm distance based on an extensive performance assessment across six dog breeds. Furthermore, an RR error of 2.58 bpm and an HR error of 7.70 bpm is achieved from a challenging distance of 100cm

The rest of this paper is organized as follows. Section II introduces the related work concerning the vital signs monitoring of dogs. Section III provides an overview of FMCW radar, while Section IV introduces the proposed pipelines encompassing both IMU-based and radar-based vital signs monitoring. The experimental setups, including the devices used and the scenarios employed in this research, are detailed in Section V. Section VI presents the results of both IMU-based and radar-based vital signs monitoring. Finally, the last section summarizes the contributions and outlines potential topics for future research.

II. Related Work

This section provides a brief overview of existing methods and related work about monitoring dogs' activities and vital signs. Furthermore, it serves as an introduction to the use of radar for vital sign monitoring with dogs.

A. Wearable-based Vital Signs Monitoring for Dog

Wearable devices designed for dogs are compact electronic accessories, often attached to the collar, equipped with sensors like accelerometers and gyroscopes to continuously monitor vital signs [1]–[3], and daily activities. Some devices include heart sensors like ECG that provide heartbeat information such as heart rate [6]–[10]. The primary advantages of wearable devices lie in their ability to offer continuous monitoring, allowing for early detection of abnormalities, changes in behavior, or potential health issues.

However, they occasionally cause discomfort for dogs, especially when the device is large and restricts their natural postures. This issue is more visible in ECG and Photoplethysmogram (PPG) based sensors, which require invasive and direct skin contact, leading to hair removal for proper electrode placement in case of ECG and better visibility of the change in skin color due to blood circulation necessary for PPG-based monitoring. Additionally, ECG requires stillness for accurate readings, and veterinarians often resort to anesthesia, straining the dogs' overall health.

B. Radar-based Vital Signs Monitoring for Dog

Radar is an electromagnetic wave-based imaging and localization technology used in many industries including healthcare. Radar can be classified based on the type of waveform it emits into two categories: The first is Continuous Wave (CW) radar [11] which also includes a variant called Frequency Modulated Continuous Wave (FMCW) [5] radar. The second category is Pulse-based radar that includes Impulse Radio Ultra-Wideband (IR-UWB) [12] and Ultra-Wideband (UWB) [4].

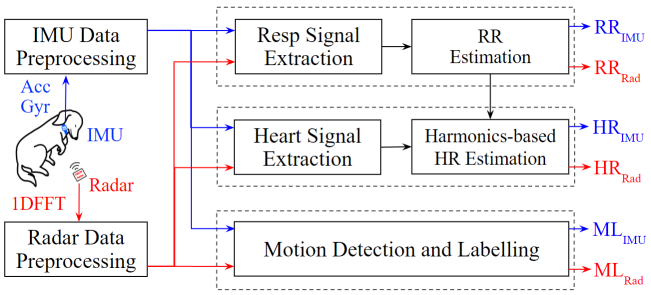

Fig. 1. Overview of Dogs' Vital Sign Monitoring Flow

III. Methodology

This section provides an overview of the proposed dogs' vital signs monitoring methodology. As illustrated in Fig. 1, the processing flow for the proposed method includes several key functional blocs. Due to challenges with using ECG and respiratory belts as ground truth for different dog types and sizes, the initial emphasis is on validating the use of IMU-based vital signs monitoring as it provides a more comfortable and easy-to-mount solution. Next, the validated IMU-based monitoring method is used as a reference for radar-based vital signs monitoring evaluation. Identical pipelines are implemented to process data from both IMU and radar for estimating the respiration and heart rates, as their measuring concept relies on the processing of the same type of physical signal that captures the body surface vibrations generated by the impact or respiration and heartbeat, also known as Seismocardiogram (SCG). An additional motion detection process is included to provide a reliability measure to the estimated vital signs by both IMU and Radar.

TABLE I
Dogs' Respiratory and Heart Rates During Sleep or Rest

Size	Weight	RR (BPM)	HR (BPM)
Small	10kg<	10 - 34	90 - 120
Medium	11kg - 26kg		70 - 110
Large & Giant	>27kg		60 - 90

A. Dogs' Vital Signs

TABLE I presents dogs' respiratory and heart rate range during sleep or rest. Normal resting respiratory rates range from 20 to 34 breaths per minute, and during sleep, it decreases to a range of 10-30 breaths per minute. Dogs' heart rates vary by size, age, and activity level. Smaller dogs and puppies generally have faster heart rates, while larger or older dogs may exhibit slower rates. Heart rates also vary with activity, being slower during sleep and increasing after exercise. Large breeds like Golden Retrievers and giant breeds such as Alaskan Malamutes have rates of 60 to 90 beats per minute, medium-sized breeds like Welsh Corgis and Australian Shepherds range from 70 to 110, and smaller breeds like Poodles and Dachshunds may have rates of 90 to 120 [13].

B. Raw Data Preprocessing

To enhance the quality and reliability of the acquired data, a preprocessing step is essential for both IMU and radar data. The data preprocessing steps for both IMU and Radar are described next.

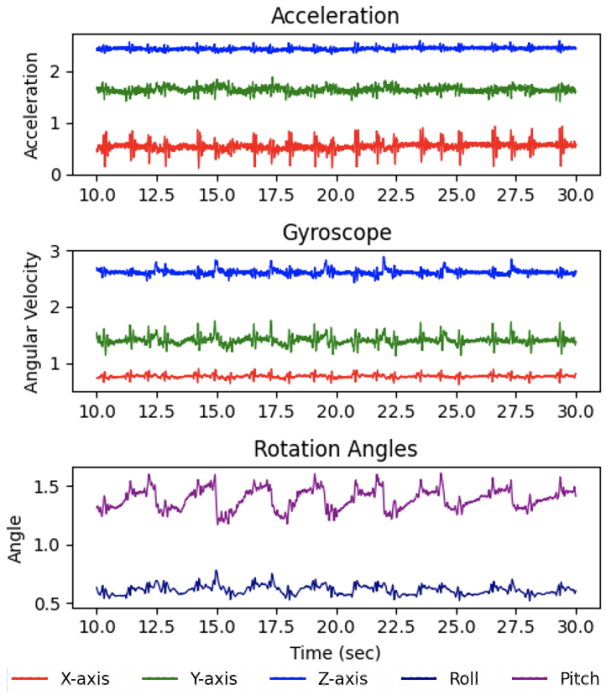

Fig. 2. IMU Preprocessed Data

1) IMU Data Preprocessing Steps: The IMU provides acceleration and gyro information across all axes (x, y, and z) as shown in Fig 2. The received data is normalized according to equation (1):

$$x^i_{norm} = \frac{x^i - x_{min}}{x_{max} - x_{min}} \tag{1}$$

where x^i represents the original value of the data point, while x_{min} and x_{max} represent the minimum and maximum values of the entire data. This scaling process confines the data within the range of 0 to 1. Dogs vary significantly in size depending on their breeds, leading to differences in acceleration and gyro data levels. Therefore, normalization becomes crucial to standardize the data and generalize the algorithm across a variety of dog sizes. A complementary filter [14] is applied next to obtain the roll (ψ) and pitch (θ) values from the acceleration and gyro data. The purpose of acquiring these signals is to perform a comparative evaluation to conclude about the best signal to use for accurate IMU-based vital signs monitoring.

2) Radar Data Preprocessing: Fig. 3 illustrates the pre-processing steps performed for FMCW radar. First, 1-dimensional FFT (1DFFT) data is generated internally by the radar board and obtained directly from its output. This data provides a spatial arrangement of the returned signals into buckets called 'Range Bins'. Static clutter is removed next by subtracting the mean value from each range bin. Subsequently, only range bins with movements will have a high magnitude. Based on this information, the chest range bin is automatically selected as the one having the highest magnitude. Following the selection of the chest range bin, the phase part of the signal at that bin is considered since it contains the details of the micro-vibrations caused by respiration and heartbeats. Since phase data is wrapped in $[-\pi, \pi]$ range, an unwrapping step is performed to obtain phase data ($\phi(n)$) that can be directly interpreted as chest displacement. Fig 4 shows a sample of the unwrapped phase signal at the output of the radar preprocessing stage.

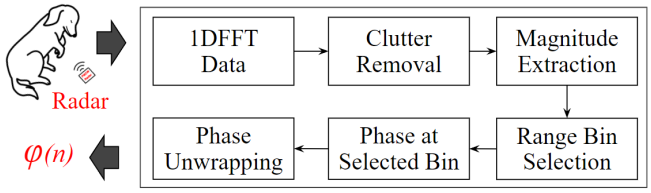

Fig. 3. Radar Data Preprocessing Pipeline

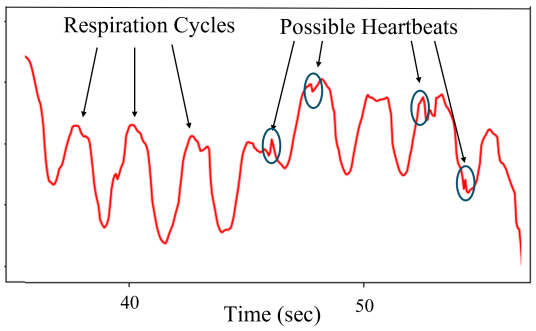

Fig. 4. Radar Preprocessed Data (Unwrapped Phase $\phi(n)$)

C. Respiration Rate Estimation Pipeline

Obtaining the respiration signal and estimating the rate from the preprocessed IMU and radar data involve following the processing sequence illustrated in Fig. 5.

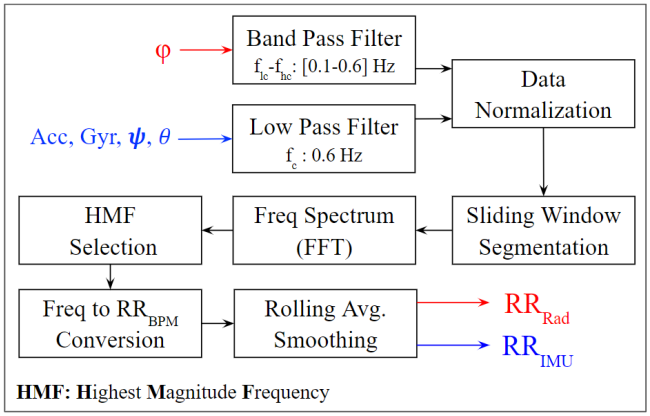

Fig. 5. Respiration Rate Estimation Pipeline

The first step involves applying a 2nd-order low-pass Butterworth filter (LPF) to the IMU preprocessed data and a 2nd-order band-pass Butterworth filter (BPF) to the unwrapped phase signal from the radar. The high cutoff frequency (f_{hc}) is set to reflect the highest respiratory rate that a subject can attain. This frequency is chosen to cover any higher respiration rates due to the subject's differences and breathing patterns. This step is performed to separate the respiration signal and attenuate the high-frequency noise from the signal. Next, a normalization step is applied using equation (1).

Once the respiration signal is separated, a sliding window segmentation is applied to divide the data into 15-second segments with a 1-second sliding time in preparation for respiration rate estimation. The window length is chosen to be long enough to capture several respiration cycles necessary for the frequency analysis used in the next step. The FFT algorithm is used on each of the signal segments to obtain the frequency spectrum, by which the respiration frequency is determined by selecting the highest magnitude frequency (HMF). The respiration rate (RR) is derived from HMF by applying equation (2) and reported as beats per minute (BPM).

$$RR(bpm) = RESP_{freq}(Hz) * 60(bpm/Hz) \quad (2)$$

The final step consists of smoothing the resulting RR signal through a 20-sec rolling average window to manage abrupt alterations and mitigate the impact of outliers that could potentially emerge because of the computational process.

D. Heart Rate Estimation Pipeline

Unlike respiration, heartbeats are more subtle and difficult to detect due to the small scale of their impact on the surface of the skin compared to respiration. To reliably extract the heartbeat signal and estimate the heart rate (HR), the pipeline depicted in Fig. 6 is implemented.

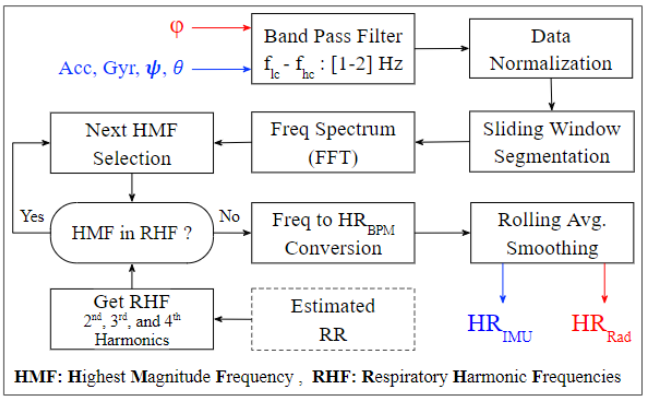

Fig. 6. Heart Rate Estimation Pipeline

The first step is extracting the heartbeat signal from the preprocessed data (for both IMU and radar) using a 2nd-order band-pass filter (BPF) with cutoff frequencies (f_{lc}) and (f_{hc}) set to cover the typical heartbeat range of the human or dog. Similar to the RR estimation pipeline, normalization is applied to scale the data within the range of 0 to 1. Fig. 7 shows the result of the respiration and heartbeat signal separation for both IMU and radar compared with their preprocessed signals.

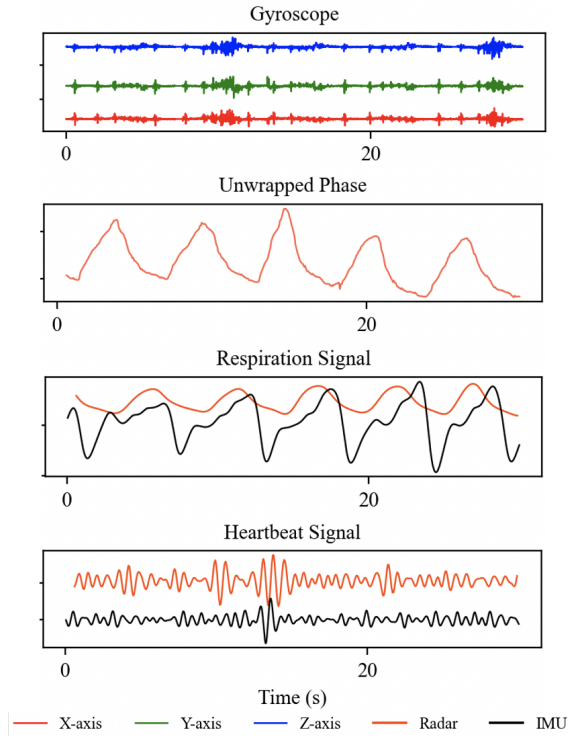

Fig. 7. Respiration and Heartbeat Signal Separation

Then, a 15-second window with a 1-second sliding time is applied to segment the normalized filtered signal in preparation for the rate estimation step. Using FFT, the frequency spectrum is inspected to select the HMF. An additional condition is applied to the selection process that involves checking if the current HMF is similar to the respiratory harmonics frequencies (RHF) that include the 2nd, 3rd, and 4th harmonics, computed based on the RR estimated previously in the respiration pipeline. In such cases, the next HMF is selected and tested again for similarity with RHF. This additional check is included since these harmonics closely resemble the heart rate signal both in terms of frequency and amplitude. This proximity and similarity in amplitude can lead to interference, resulting in errors in heart rate measurements that are challenging to filter out.

After skipping the respiration harmonics frequencies, the frequency with the highest magnitude (HMF) in the remaining signal frequencies is selected. It is next converted into a bpm value using equation (2). The final HR values are the result of applying a 20-second window-based rolling average to get the final HR values.

E. Motion Detection and Labelling

Unlike previous studies, a motion detection and labelling function is included aimed at complementing the measured

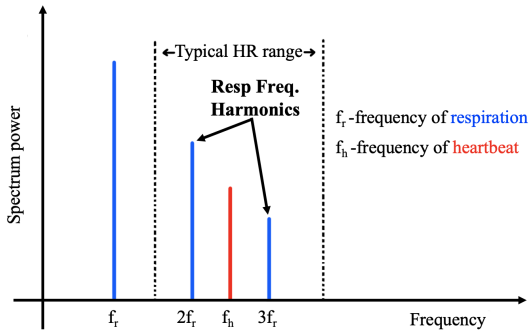

Fig. 8. Breathing Harmonics Impact on Heartbeat Frequency Estimation

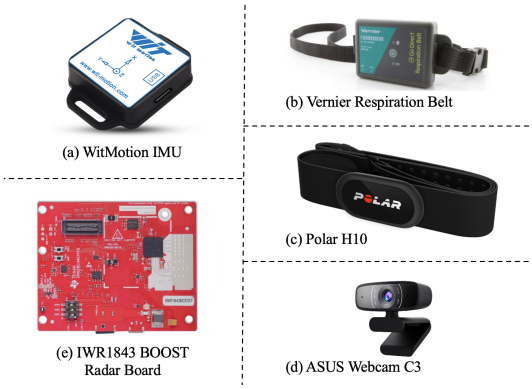

Fig. 9. Devices Used to Collect Data

vital signs with a reliability measure to evaluate the trustworthiness of the monitoring results. This task is conducted in parallel with the vital signs estimation and used to evaluate the subject motion state, allowing to focus on segments of the signal where the subject is idle, an ideal condition to provide reliable measurement.

IV. Hardware Setup and Experimental Protocol

To validate the performance of the proposed vital sign monitoring approach, a series of experiments are conducted using both an FMCW radar and reference devices with multiple dog subjects.

A. Experimental Hardware Description

Fig. 9 shows the devices used in the experiment for vital signs monitoring. The Witmotion IMU sensor has a 3-axis accelerometer and a 3-axis gyroscope. It transmits the data using a Bluetooth connection and weighs only 16 grams with dimensions of less than 5cm on each side, placing less stress on dogs. In these experiments, it is placed on dogs' collars and set up to collect data at a sampling rate of 200Hz. To provide respiration reference data, a Vernier Respiration Belt is used with a sampling frequency of 20Hz. It is attached to the dog's stomach and collects the change of exerted force on the belt when inhaling and exhaling. In the case of heartbeat, a Polar H10 strap was used to collect ECG reference data. The data collection rate is 130Hz and reports both ECG and HR values accurately. Since the dogs have hair on their chest, which is difficult to remove, a gel was applied to the electrodes on the Polar H10, and a double-loop configuration was utilized to secure it tightly to the subject. Every experiment was recorded using the web camera shown in Fig. 9 (d).

The FMCW radar board used is the IWR1843BOOST from Texas Instrument (TI), operating in the frequency range of 77-81GHz. The radar includes four receivers three transmitters and a dedicated Digital Signal Processor (DSP) for advanced internal computations. The sampling rate is set to 16Hz with a range resolution of 9cm.

B. Details of Experimental Protocol

Since different devices are used for IMU-based monitoring and radar-based monitoring, the experiments were conducted separately.

1) IMU-based Experiment: The left side of Fig. 10 shows the experiment scene for IMU-based vital signs monitoring. Since the size of reference devices was big for the dog, it was necessary to conduct separate experiments for respiratory rate and heart rate. This approach was adopted to prevent any discomfort for the dogs during sleep. In the left upper picture of Fig. 10, the experimental setup for respiratory rate is depicted. The IMU sensor was positioned on the collar, and a respiration belt was placed around the stomach. The left lower picture illustrates the experimental arrangement for heart rate. Similar to the respiratory rate experiment, the IMU sensor was attached to the collar, and the Polar device was positioned on the chest with the application of gel to the electrodes. Each session lasted for 1 to 3 minutes and was recorded multiple times. A series of recording sessions were conducted while the dog was asleep. To evaluate the accuracy of our estimated vital signs, the Vernier respiration belt and Polar H10 were used to establish a ground truth for respiratory rate and heart rate.

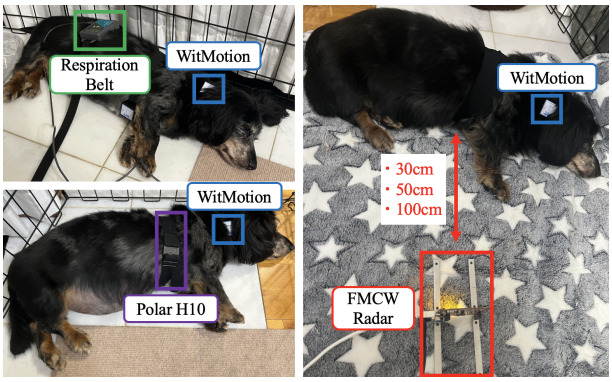

Fig. 10. Experiment Scenes

2) Radar-Based Experiment: The right side of Fig. 10 shows the experiment scene for Radar-based vital signs monitoring. The IMU sensor was positioned on the collar, and an FMCW radar was placed 30cm, 50cm, or 100cm away from the dog's chest. Each session lasted 1 to 3 minutes and was recorded multiple times. A series of recording sessions were conducted while the dog was asleep. To evaluate the accuracy of the estimated vital signs, respiratory rate and

heart rate estimated using the IMU were used as the ground truth. From the results of IMU-based vital signs estimation, pitch value and x-axis gyro were used to obtain the ground truth for respiratory rate and heart rate, respectively.

3) Subjects Participated in Experiment: The dog subjects used in both IMU-based and radar-based experiments were shown in TABLE II. As discussed in section IV, dogs exhibit respiratory rates ranging from 10 to 34 breaths per minute across all breeds. Consequently, the cutoff frequency for respiration was established between 0.1 Hz and 0.6 Hz. However, determining the appropriate cutoff frequency for heart rate poses challenges due to variations in heart rates among different age groups and breeds. Typically, younger dogs have higher heart rates than the average adult, while older dogs tend to have lower rates. In this research, the TABLE II illustrates that larger dogs, such as subjects number 5 and 6, are relatively young and have higher heart rates than the average, whereas smaller dogs, like subjects number 3 and 4, are relatively old and have lower heart rates. To accommodate this variability, a universal cutoff frequency for heart rate was set at 1.0 to 2.0Hz, covering a range of 60 to 120 beats per minute. This range aims to encompass the diverse heart rates observed in dogs of various breeds and ages.

TABLE II
DOG SUBJECTS INFORMATION

Subject Num.	Breeds	Gender	Age	Weight (kg)
1	Chihuahua	Male	2	3
2	Poodle	Male	9	4
3	Dachshund	Female	17	7
4	Shiba Inu	Female	11	12
5	Labradoodle	Male	2	17
6	Golden Retriever	Female	3	28

V. EVALUATIONS OF ESTIMATED RR AND HR

This section describes the results of vital signs estimation using both IMU and radar in time segments labeled as "Idle" by the motion detection and labelling bloc. Firstly, the results of IMU-based vital signs estimation were assessed in comparison with reference devices. Subsequently, the radar-based results were evaluated using IMU with the optimal axis for each respiratory and heart rate estimation. Mean absolute error (MAE) was employed to assess the results from both IMU and radar, with its calculation defined by equation 3, where y_i represents the prediction and x_i represents the true value.

$$MAE = \frac{\sum_{i=1}^{n} |y_i - x_i|}{n} \tag{3}$$

A. IMU-Based Results

The results of IMU-based vital signs estimation are provided in this subsection.

1) Respiratory Rate Estimation: Fig. 11 shows a sample of the results of the respiration wave obtained from both the IMU and the respiration belt, and the wave patterns are shown clearly. Similar to the IMU-based respiratory rate estimation, to obtain the ground truth for respiratory rate, a 15-second window with a 1-second sliding time was applied to segment the signal obtained from the respiration belt. FFT was then applied to all windows to calculate the respiratory rate.

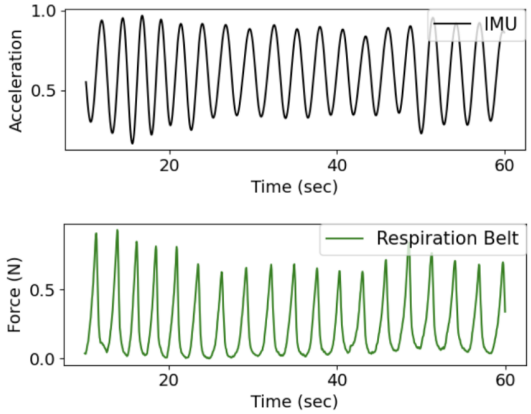

Fig. 11. Sample Respiration Signals from IMU and Respiration Belt

TABLE III provides a comparison between the results of respiratory rate (RR) estimation using 2nd-order and 4th-order low-pass filter and the 3-axis accelerometer (ACC), 3-axis gyroscope (GYR), roll ψ, and pitch (θ). Subject number 3 and 4 participated in the experiment for respiratory rate estimation. The best MAE of 0.24 was achieved with pitch when applying a 2nd-order low-pass filter, making it suitable as a reference device for respiration measurement. Furthermore, when using a 2nd-order low-pass filter, a MAE of 0.49 was obtained with gyro, while acceleration resulted in a MAE of 1.87. Gyroscopes achieved superior results in all three axes compared to accelerometers when using a 2nd-order low-pass filter. This difference was happened because accelerometers are sensitive to changes in linear acceleration, making them prone to interference from motion. However, gyroscopes measure angular velocity, which may result in less sensitivity to motion but accurate detection of rotational movement associated with respiration. Since respiration movement contains both linear and rotational components, the fusion of acceleration and gyro resulted in better performance than using a single sensor.

When comparing the results between the 2nd-order and 4th-order low-pass filters, the 2nd-order filter produced better results for gyro, while the 4th-order filter yielded better results for acceleration. Since the gyro is often associated with lower-frequency components, especially when measuring slower motions such as those related to breathing, it might carry respiratory-related information without requiring a high-order filter. However, acceleration signals may exhibit both lower-frequency components related to the overall motion of the body and higher-frequency components associated with respiratory-induced chest movements during

TABLE III
MAE OF IMU-BASED RR AND HR ESTIMATION (BPM)

Filter		2nd-Order			4th-Order		
		RR	**HR**	**HR_BHR**	**RR**	**HR**	**HR_BHR**
X	Acc	1.68	13.55	8.07	1.38	12.02	9.81
	Gyr	0.72	9.82	**4.89**	2.48	9.08	6.96
Y	Acc	1.75	10.5	5.97	1.19	9.64	7.50
	Gyr	0.51	12.93	7.53	1.21	11.78	9.26
Z	Acc	2.17	14.08	7.68	1.44	11.99	9.75
	Gyr	0.25	11.61	7.02	0.70	10.34	8.94
Roll (ψ)		0.74	10.33	7.59	0.90	11.73	8.48
Pitch (θ)		**0.24**	11.31	9.18	0.32	12.32	10.01

*RR results are based on 2 dogs across 32 sessions.
*HR results are based on 1 dog across 12 sessions.

breathing measurements. Therefore, using a 4th-order filter for acceleration signals could be preferable as it selectively captures and emphasizes the higher-frequency components associated with respiratory-induced chest movements while attenuating unwanted components and noise.

2) Heart Rate Estimation: Fig. 12 shows a sample of the result of the heartbeat estimation process using IMU and ECG signal from Polar H10. The ground truth for heart rates was automatically calculated by Polar H10 based on ECG data. Due to the challenges and instability associated with ECG, only subject number 3 participated in the experiment for heart rate estimation. The result of heart rate with breathing harmonics removal (HR_BHR) is also shown in TABLE III.

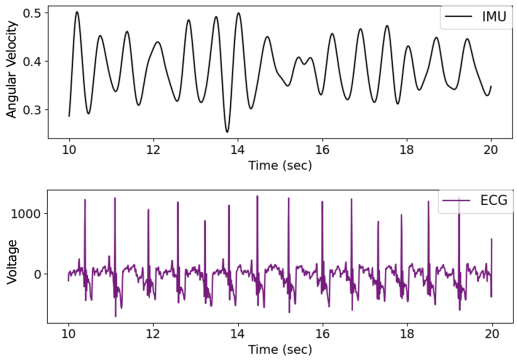

Fig. 12. Sample Heartbeat Signals from IMU and ECG

Fig. 13 illustrates the impact of breathing harmonics on heart rate estimation. The black line represents the estimated heart rate from IMU, the purple line indicates the ground truth for heart rate, and the red rectangles show where breathing harmonics affect the heart rate estimation using IMU. The upper graph displays the heart rate estimated result without considering harmonics, while the lower graph shows the result after removing breathing harmonics. The outliers were eliminated, resulting in smoother heart rates and lower MAE. The impact of breathing harmonics removal (HR_BHR) on the results is presented in TABLE III, demonstrating notable improvement across both sensors.

TABLE III also provides a comparison between the results

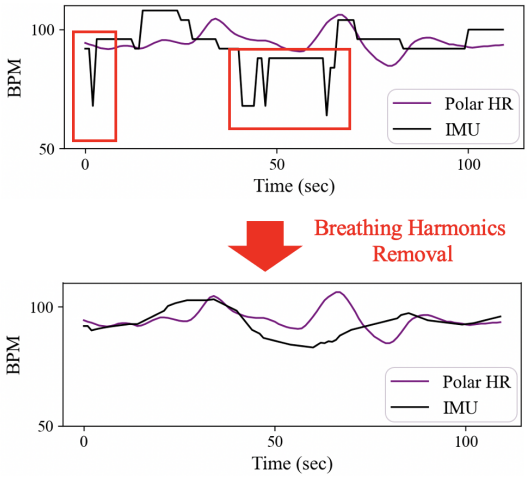

Fig. 13. Breathing Harmonics Impact on HR Estimation (IMU)

of heart rate (RR) estimation using 2nd-order and 4th-order band-pass filter and the 3-axis accelerometer (ACC), 3-axis gyroscope (GYR), roll (ψ), and pitch (θ). The results for estimating heart rate with breathing harmonics removal demonstrate good performance, achieving an MAE of 4.89 bpm when using a 2nd-order band-pass filter and the x-axis of the gyroscope across 12 sessions held on three different days. The gyroscope performed slightly better than acceleration in both the 2nd and 4th-order band-pass filters, with MAEs of 7.24 bpm and 6.48 bpm for acceleration and gyro when using the 2nd-order band-pass filter, and 9.02 bpm and 8.29 bpm when using the 4th-order band-pass filter. This superiority can be attributed to the fact that accelerometers are highly sensitive to changes in linear acceleration, making them susceptible to interference from motion. As the heartbeat signal is much smaller than the motion signal, extracting the heartbeat signal from the accelerometer may become challenging due to interference from motion signals. Roll and pitch were found suitable for measuring respiratory rate, but as they represent orientation changes, they may lack sensitivity to the specific movements associated with heartbeats. Consequently, they can be influenced by other body movements or gravitational effects, potentially leading to less accurate heart rate measurements.

When comparing the results between the 2nd-order and 4th-order band-pass filters, the 2nd-order achieved better results for both acceleration and gyro. This may be because heart rate signals are periodic and sensitive to phase distortions, and a 2nd-order filter may introduce less phase distortion compared to a 4th-order filter, making it more suitable for preserving the phase relationships associated with heart rate cycles.

B. Radar-Based Results

The results of radar-based vital signs estimation are provided in this subsection.

1) Respiratory Rate Estimation: Fig. 14 shows a sample of the results of the respiration wave obtained from radar and the ground truth using subject 3, and the wave patterns

are shown clearly. To obtain the ground truth for respiratory rate, the same process with a 2nd-order low-pass filter was applied to the pitch values data obtained from the IMU, which was obtained simultaneously with the radar data.

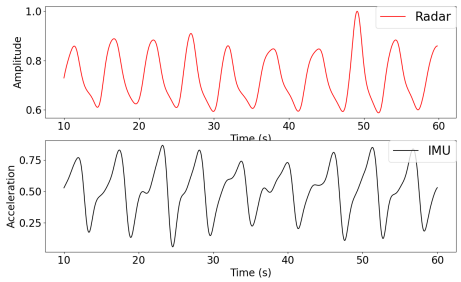

Fig. 14. Sample Respiration Signals from Radar and IMU

TABLE IV shows a comparison of the average MAE between the estimated respiratory rate and heart rate using 2nd-order or 4th-order at three different distances (30cm, 50cm, and 100cm) of the radar. The best MAE of 2.40 was obtained using a 2nd-order band-pass filter when the radar was placed 50cm away from the dogs' chest, while the worst MAE of 3.09 was observed using a 4th-order band-pass filter at a distance of 30cm. When the radar is too close to the subject, small movements and vibrations can introduce motion artifacts, negatively impacting signal quality. Consequently, the results at 30cm were inferior compared to other distances. As the radar moves farther from the subject, motion artifacts weaken, but the signals of vital signs also get weaker. Therefore, the results at 50cm were slightly better than those at 100cm.

TABLE IV
MAE OF RADAR-BASED RR AND HR ESTIMATION (BPM)

Filter	2nd-Order			4th-Order		
	RR	HR	HR_BHR	RR	HR	HR_BHR
30cm	2.95	9.08	9.05	3.09	9.99	9.97
50cm	**2.40**	7.10	**6.90**	2.47	7.56	7.31
100cm	2.58	7.77	7.70	2.75	8.69	8.60

*30cm and 50cm results are based on 2 dogs across 16 sessions.
*100cm result is based on 5 dogs across 26 sessions.

When comparing the results between the 2nd-order and 4th-order band-pass filters, the 2nd-order achieved better results than the 4th-order band-pass filter. This may be attributed to the fact that noise from movement or the surrounding environment is predominantly in a lower frequency range. Therefore, a 2nd-order band-pass filter proves effective in filtering out this noise. Higher-order filters may provide better noise rejection, but they also introduce more phase distortion.

2) Heart Rate Estimation: Fig. 15 shows a sample of the results of the heartbeat waves obtained from radar and the ground truth using subject 3, and the wave patterns are shown clearly. To obtain the ground truth for heart rate, the same process with a 2nd-order band-pass filter was applied to the x-axis gyro data obtained from the IMU, which was obtained simultaneously with the radar data.

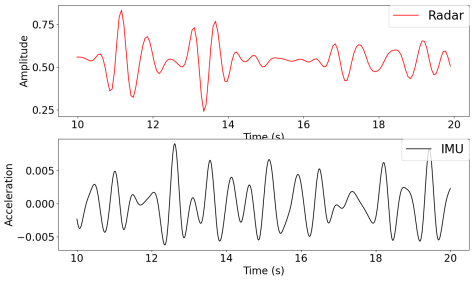

Fig. 15. Sample Heartbeat Signals from Radar and IMU

Fig. 16 illustrates the impact of breathing harmonics on heart rate estimation. The red line represents the estimated heart rate from radar, the black line indicates the ground truth for heart rate from IMU, and the red rectangles show where breathing harmonics affect the heart rate estimation using radar. The upper graph displays the heart rate estimated result without considering harmonics, while the lower graph shows the result after removing breathing harmonics. The outlier was eliminated, resulting in smoother heart rates and lower MAE. The impact of breathing harmonics removal (HR_BHR) on the results is presented in TABLE IV, demonstrating improvement across all distances.

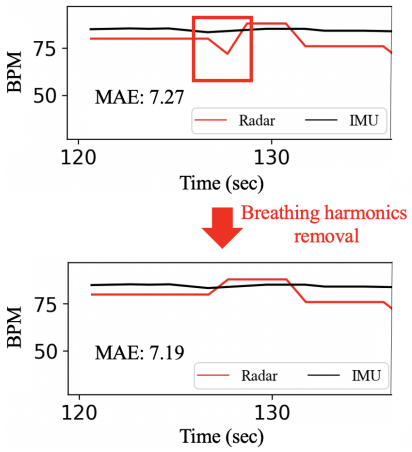

Fig. 16. Breathing Harmonics Impact on HR Estimation (Radar)

From TABLE IV, similar to the results of respiratory rate estimation, the best average MAE of 6.90 was obtained for heart rate estimation using a 2nd-order band-pass filter when the radar was placed 50cm away from the dogs' chest across 16 sessions with two different dog subjects. Conversely, the worst average MAE of 9.97 was observed using the 4th-order band-pass filter at a distance of 30cm across 16 sessions with two dog subjects. Considering that the displacement of heartbeats is much smaller than the displacement of respiration, the heartbeat signals are inherently weaker than the respiratory signals. As a result, motion artifacts have a more pronounced impact on the estimation

of heart rate, leading to notable differences in the results for distances of 30cm, 50cm, and 100cm.

Similarly to respiratory rate estimation, the use of a 2nd-order band-pass filter yielded better results compared to a 4th-order band-pass filter. This may be because heart rate signals are periodic and sensitive to phase distortions, and a 2nd-order filter may introduce less phase distortion compared to a 4th-order filter, making it more suitable for preserving the phase relationships associated with heart rate cycles.

3) Impact of Postures: To assess the accuracy of vital signs estimation in various postures, experiments were conducted at a distance of 100cm with four different postures (sleeping, lying down, sitting, and standing). These postures are commonly assumed by dogs. If the dog's head was on the floor, the posture was categorized as sleeping, and if not, it was categorized as lying down. Five dog subjects participated in the experiments with the sleeping posture, while four dog subjects participated in the experiments with other postures.

TABLE V
COMPARISON BETWEEN THE DOGS' POSTURES AT 100CM (BPM)

Posture	Num. of Dogs	Num. of Sess.	RR	HR_BHR
Sleeping	5	26	**2.59**	**7.70**
Lying Down	4	10	3.78	9.73
Sitting	4	10	4.44	9.74
Standing	4	10	4.67	12.61

TABLE V presents the MAE for different postures obtained using a 2nd-order band-pass filter. Overall, the performance degrades for lying down, sitting, and standing posture. Dogs exhibited uncontrollable behavior during recordings, and even in sitting or lying down postures, they displayed subtle movements like moving their head or wagging their tail. In standing postures, larger movements such as stepping occurred. Additionally, the radar is highly sensitive to even small movements, contributing to decreased accuracy when postures involve more movement.

VI. CONCLUSION AND FUTURE WORK

This research introduced a processing pipeline designed to estimate both respiration and heart rates using IMU and FMCW radar technologies. The key contributions of this research include (1) the proposal of an improved vital sign estimation method for dogs through the elimination of breathing harmonics used by both radar and IMU, (2) validation of the use of IMU sensors as vital signs monitoring reference, and (3) evaluation of radar results using an IMU sensor with multiple dog subjects, encompassing different breeds, sizes, and ages. Notably, an average error of 2.40 bpm for respiratory rate and 6.90 bpm for heart rate was achieved across two different dog subjects when the radar was positioned 50 cm away from the dogs' chest. Even with five different dog subjects, an average error of 2.58 bpm for respiratory rate and 7.70 bpm for heart rate was attained when the radar was positioned at 100cm. These results underscore the reliability and adaptability of our approach across diverse breeds, sizes, and ages of dogs.

While the outcomes of this study are certainly promising, there are significant limitations that warrant attention in future research endeavors. Our current focus on monitoring vital signs in dogs necessitates validation on a broader and more diverse sample of dogs, encompassing various breeds and sizes. Additionally, for heart rate measurements, it is crucial to explore more accurate signals, such as ECG, especially in veterinarian settings. Another notable limitation of our current processing pipeline is its inability to measure respiratory rate and heart rate accurately when dogs are in motion. Addressing these limitations will enhance the applicability and robustness of our approach.

REFERENCES

[1] M. Foster, J. Wang, E. Williams, D. Roberts, and A. Bozkurt, "ECG and respiration signal reconstruction from an IMU at various orientations during rest or sleep for dog welfare monitoring," in *Proceedings of the 8th International Conference on Animal-Computer Interaction*, 2021.

[2] M. Foster, J. Wang, E. Williams, D. L. Roberts, and A. Bozkurt, "Inertial measurement based heart and respiration rate estimation of dogs during sleep for welfare monitoring," in *Proceedings of the Seventh International Conference on Animal-Computer Interaction*. Association for Computing Machinery, 2021.

[3] J. Wang, M. Foster, A. Bozkurt, and D. L. Roberts, "Motion-resilient ECG signal reconstruction from a wearable IMU through attention mechanism and contrastive learning," in *Proceedings of the Ninth International Conference on Animal-Computer Interaction*, 2022.

[4] W. Pengfei, M. Yangyang, L. Fulai, Z. Yang, Y. Xiao, L. Zhao, A. Qiang, L. Hao, and W. Jianqi, "Non-contact vital signs monitoring of dog and cat using a UWB radar," *Animals*, vol. 10, no. 2, 2020.

[5] H. Yang, Y. Luo, A. Qi, M. Miao, and Y. Qi, "FMCW-radar-based vital-sign monitoring of pet," in *2021 13th International Symposium on Antennas, Propagation and EM Theory (ISAPE)*, vol. 1, 2021.

[6] R. Brugarolas, T. Latif, J. Dieffenderfer, K. Walker, S. Yuschak, B. L. Sherman, D. L. Roberts, and A. Bozkurt, "Wearable heart rate sensor systems for wireless canine health monitoring," *IEEE Sensors Journal*, vol. 16, no. 10, pp. 3454–3464, 2016.

[7] H. Jarkoff, G. Lorre, and E. Humbert, "Assessing the accuracy of a smart collar for dogs: Predictive performance for heart and breathing rates on a large scale dataset," *bioRxiv*, 2023.

[8] V. S. Jonckheer-Sheehy, C. M. Vinke, and A. Ortolani, "Validation of a polar® human heart rate monitor for measuring heart rate and heart rate variability in adult dogs under stationary conditions," *Journal of Veterinary Behavior*, vol. 7, no. 4, 2012.

[9] M. Foster, R. Brugarolas, K. Walker, S. Mealin, Z. Cleghern, S. Yuschak, J. C. Clark, D. Adin, J. Russenberger, M. Gruen, B. L. Sherman, D. L. Roberts, and A. Bozkurt, "Preliminary evaluation of a wearable sensor system for heart rate assessment in guide dog puppies," *IEEE Sensors Journal*, vol. 20, no. 16, pp. 9449–9459, 2020.

[10] O. Lahdenoja and et al., "Cardiac monitoring of dogs via smartphone mechanocardiography: a feasibility study," *BioMedical Engineering OnLine*, vol. 18, no. 1, pp. 1–14, 2019.

[11] Y. Xiao, Y. Yue, L. Hao, Z. Yang, L. Fulai, and W. Pengfei, "Non-contact determination of vital signs monitoring of animals in hemorrhage states using bio-radar," *Progress In Electromagnetics Research M*, vol. 100, 2021.

[12] P. Wang, Y. Zhang, Y. Ma, F. Liang, Q. An, H. Xue, X. Yu, H. Lv, and J. Wang, "Method for distinguish humans and animals in vital signs monitoring using ir-uwb radar," *International Journal of Environmental Research and Public Health*, vol. 16, no. 22, 2019.

[13] D. Stott. "what are considered normal heart rates, breathing rates, and temperature in dogs?". [Online]. Available: https://wagwalking.com/wellness/what-are-considered-normal-heart-rates-breathing-rates-and-temperature-in-dogs/

[14] R. G. Valenti, I. Dryanovski, and J. Xiao, "Keeping a good attitude: A quaternion-based orientation filter for IMUs and MARGs," *Sensors*, vol. 15, no. 8, pp. 19 302–19 330, 2015.